

Ultra-Small Plutonium Oxide Nanocrystals: An Innovative Material in Plutonium Science

Damien Hudry,^{*,[a]} Christos Apostolidis,^[a] Olaf Walter,^[a] Arne Janßen,^[a] Dario Manara,^[a] Jean-Christophe Griveau,^[a] Eric Colineau,^[a] Tonya Vitova,^[b] Tim Prüßmann,^[b] Di Wang,^[c] Christian Kübel,^[c] and Daniel Meyer^[d]

Abstract: Apart from its technological importance, plutonium (Pu) is also one of the most intriguing elements because of its non-conventional physical properties and fascinating chemistry. Those fundamental aspects are particularly interesting when dealing with the challenging study of plutonium-based nanomaterials. Here we show that ultra-small (3.2 ± 0.9 nm) and highly crystalline plutonium oxide (PuO_2) nanocrystals (NCs) can be synthesized by the thermal decomposition of plutonyl nitrate ($[\text{PuO}_2(\text{NO}_3)_2] \cdot 3 \text{H}_2\text{O}$) in a highly coordinating organic medium. This is the first example reporting on the preparation of significant quantities (several tens of milligrams) of PuO_2 NCs, in a controllable

and reproducible manner. The structure and magnetic properties of PuO_2 NCs have been characterized by a wide variety of techniques (powder X-ray diffraction (PXRD), X-ray absorption fine structure (XAFS), X-ray absorption near edge structure (XANES), TEM, IR, Raman, UV/Vis spectroscopies, and superconducting quantum interference device (SQUID) magnetometry). The current PuO_2 NCs constitute an innovative material for the study of challenging problems as diverse as the transport behavior of plutonium in the environment or size and shape effects on the physics of transuranium elements.

Introduction

Because of its unconventional physical properties^[1] and fascinating chemistry,^[2] plutonium (Pu) is probably one of the most intriguing elements within the periodic table. Innovative materials based on plutonium are highly interesting both for fundamental and applied research. However, radiological and chemical plutonium toxicities combined with its low availability are major obstacles that slow down this fascinating research and render the process of discovering innovative plutonium-based materials highly challenging.

The size reduction down to few nanometers (i.e., the synthesis of plutonium-based nano-objects) constitutes an interesting approach to produce new plutonium materials. Indeed, nanocrystals (NCs) represent fundamental building blocks in nanoscience and nanotechnology because of their size and shape-dependent properties.^[3] Investigations and developments related to NCs have reached a high level of understanding and complexity when dealing with stable elements and led to high achievements in fields as diverse as electronics and optoelectronics,^[4] energy conversion,^[5] magnetic storage,^[6] or nanomedicine.^[7] Comparatively, fewer results have been produced within the actinide series. Whereas several authors reported on various thorium and uranium nano-objects,^[8] the lack of knowledge is particularly critical for transuranium elements.^[9]

The case of plutonium is particularly interesting because of its major technological interest. For example, the migration of plutonium in the environment is of major concern to the safety assessment of nuclear waste disposal and legacy contamination sites (nuclear accidents, for example, Chernobyl and Fukushima or atmospheric nuclear weapons testing). Indeed, experimental results about field sites (e.g., the former Nevada Test Site in the United States of America or the Mayak Production Association in Russia) showed that plutonium migrated significant distances in the subsurface much faster than predicted.^[10] The observed results clearly indicate that there is not a single process explaining the plutonium transport. Recently, the importance of colloid-facilitated transport of plutonium and other actinides gained acceptance. As a consequence, the last two decades have seen a growing research in-

[a] Dr. D. Hudry, Dr. C. Apostolidis, Dr. O. Walter, Dr. A. Janßen, Dr. D. Manara, Dr. J. C. Griveau, Dr. E. Colineau
Institute for Transuranium Elements
European Commission Joint Research Center
P.O. Box 2340, 76125 Karlsruhe (Germany)
E mail: damien.hudry@gmail.com

[b] Dr. T. Vitova, T. Prüßmann
Institute for Nuclear Waste Disposal
Karlsruhe Institute of Technology
P.O. Box 3640, 76021 Karlsruhe (Germany)

[c] Dr. D. Wang, Dr. C. Kübel
Institute of Nanotechnology/Karlsruhe Nano Micro Facility
Karlsruhe Institute of Technology, Hermann von Helmholtz Platz 1
76344 Eggenstein Leopoldshafen (Germany)

[d] Dr. D. Meyer
Institut de Chimie Séparative de Marcoule
UMR 5257, BP 17171, 30207 Bagnols sur Cèze Cedex (France)

terest on intrinsic colloids, pseudo-colloids and multicomponent systems.^[11]

For example, studies focused on intrinsic plutonium colloids extending into the nanoscale dedicated to their synthesis, structural characterization and properties were reported.^[12] Although such intrinsic colloids, sometimes referred to as plutonium nanoparticles or plutonium nanocolloids, are similar in terms of size and crystallinity to modern NCs, the degree of knowledge with plutonium is still far from the one reached with stable elements. As a consequence, a reliable and reproducible method dedicated to the controlled synthesis of plutonium-based NCs is highly desirable

In this article, we report for the first time on the controlled and quantitative synthesis of ultra-small (3.2 ± 0.9 nm) plutonium oxide (PuO_2) NCs. PuO_2 NCs were synthesized according to a non-aqueous technique and characterized by using powder X-ray diffraction (PXRD), X-ray absorption fine structure (XAFS), transmission electron microscopy (TEM) as well as infrared (IR), Raman and ultraviolet/visible (UV/Vis) spectroscopy. The reported PuO_2 NCs constitute fundamental and versatile building blocks that can be used for various purposes in future studies. As an example, the magnetic properties of the as-prepared PuO_2 NCs have been characterized by superconducting quantum interference device (SQUID) magnetometry.

Results and Discussion

PuO_2 NCs were synthesized by the thermal decomposition method in a highly coordinating organic medium.^[13] This method was already applied for thorium and uranium oxides^[8a,b] as well as to their corresponding solid solutions^[14] and recently extended to the first transuranium element namely neptunium.^[9] Because actinyl (AnO_2^{2+} with $\text{An}=\text{U}, \text{Np}$) nitrates were found as being suitable precursors for the synthesis of actinide oxide (AnO_2) NCs, the synthesis was extended for the first time to plutonium using plutonyl nitrate ($(\text{PuO}_2(\text{NO}_3)_2) \cdot 3\text{H}_2\text{O}$) as a starting plutonium precursor. The latter, dissolved in a mixture of benzyl ether (BnOBn), oleic acid (OA), and oleylamine (OAm) was thermally treated at 280°C for 30 min. The dissolution of plutonyl nitrate is facilitated by a ligand exchange reaction between nitrate and oleate anions. Subsequently, an aminolysis reaction might be involved in the formation of the plutonium oxide network as reported by several authors with stable elements.^[15] During the thermal treatment, the mixture turned from a dark-red to dark-green color (the Supporting Information, Figure S1). After cooling, an olive-green precipitate was isolated from the raw solution. The extracted precipitate was easily dispersible in apolar solvents such as toluene. Depending on the characterization technique, either the dispersed precipitate in toluene or the powder (i.e., dried precipitate) was used. Details about the synthesis, extraction procedure, and characterization techniques are given in the Supporting Information.

X-ray diffraction and absorption spectroscopy

The extracted olive-green precipitate was first characterized by PXRD at room temperature. The corresponding experimental pattern is shown in Figure 1 a along with the result of the Rietveld refinement. The observed reflections are in good agreement with the ones of bulk plutonium dioxide (PuO_2). The crystallographic structure of the latter was used to carry out the Rietveld refinement. Bulk PuO_2 crystallizes in the cubic (fcc) fluorite structure (space group $Fm\text{-}3m$) with two atoms per unit cell and a cell parameter a_{bulk} of 5.396 \AA .^[16] Both plutonium and oxygen atoms occupy special positions (0,0,0) and (0.25,0.25,0.25), respectively. As a consequence, only few parameters can be refined. Using the fundamental approach,^[17] only parameters with a real physical meaning were refined namely the cell parameter (a_{nano}), the crystallite size (C_{size}) and the isotropic atomic displacement parameters (U_{iso} ; Figure 1 b). The calculated PXRD pattern (black solid line) fits well with the experimental one (red spheres; Figure 1 a). A cell parameter a_{nano} of $5.3940(7) \text{ \AA}$ was determined along with an average crystallite size of 2 nm. The Pu–O and Pu–Pu distances calculated are $2.3357(2)$ and $3.8141(4) \text{ \AA}$, respectively. The crystallographic structure of the PuO_2 NCs derived from the Rietveld refinement is given as an inset in Figure 1 a. The value determined for the cell parameter indicates that the stoichiometry is very close to the ideal one (i.e., $\text{PuO}_{2.00}$).^[18] Recently, conflicting reports were published about the formation of hyper-stoichiometric PuO_{2+x} (with x up to 0.26).^[19] Although the formation of such a hyper-stoichiometric oxide is only possible with water at moderate temperature, the starting oxidation state of plutonium (i.e., VI) as well as the small size (i.e., high surface-to-volume ratio) of the NCs could help to stabilize PuO_{2+x} . Hence, the as-prepared PuO_2 NCs were characterized by extended X-ray absorption fine structure (EXAFS) and X-ray absorption near edge structure (XANES).

The plutonium L_3 edge Fourier transformed EXAFS (FT-EXAFS) spectrum of the as-prepared PuO_2 NCs shown in Figure 1 c clearly displays a peak at about 3.7 \AA (not phase corrected) describing the scattering of the photo-electron from the plutonium atoms in the second coordination sphere. The high-intensity of this peak and the overall similarity of the PuO_2 NCs to the bulk PuO_2 FT-EXAFS (the Supporting Information, Figure S2a) suggest a high-degree of local structural order around the absorbing plutonium atom. The best fit to the plutonium L_3 edge FT-EXAFS spectrum implies no reduction within the error bars of the 8 O atoms, that is, (6.6 ± 0.8) O atoms coordinated to Pu in the first coordination sphere (peak at about 1.8 \AA in Figure 1 c), whereas a slight reduction of the Pu coordination number from 12 to 8.1 ± 1.5 is found (see the Supporting Information for details on the fitting procedure and Figure S2 as well as Table S1). The lower Pu–Pu coordination is in agreement with the small size of the particles since the high surface-to-volume ratio leads to a large number of Pu atoms close to the surface coordinating to less than twelve plutonium atoms. The Pu–O distance determined by the EXAFS analysis ($2.31 \pm 0.01 \text{ \AA}$) is slightly shorter ($0.03 \pm 0.01 \text{ \AA}$) than the distance calculated with the cell parameters deter-

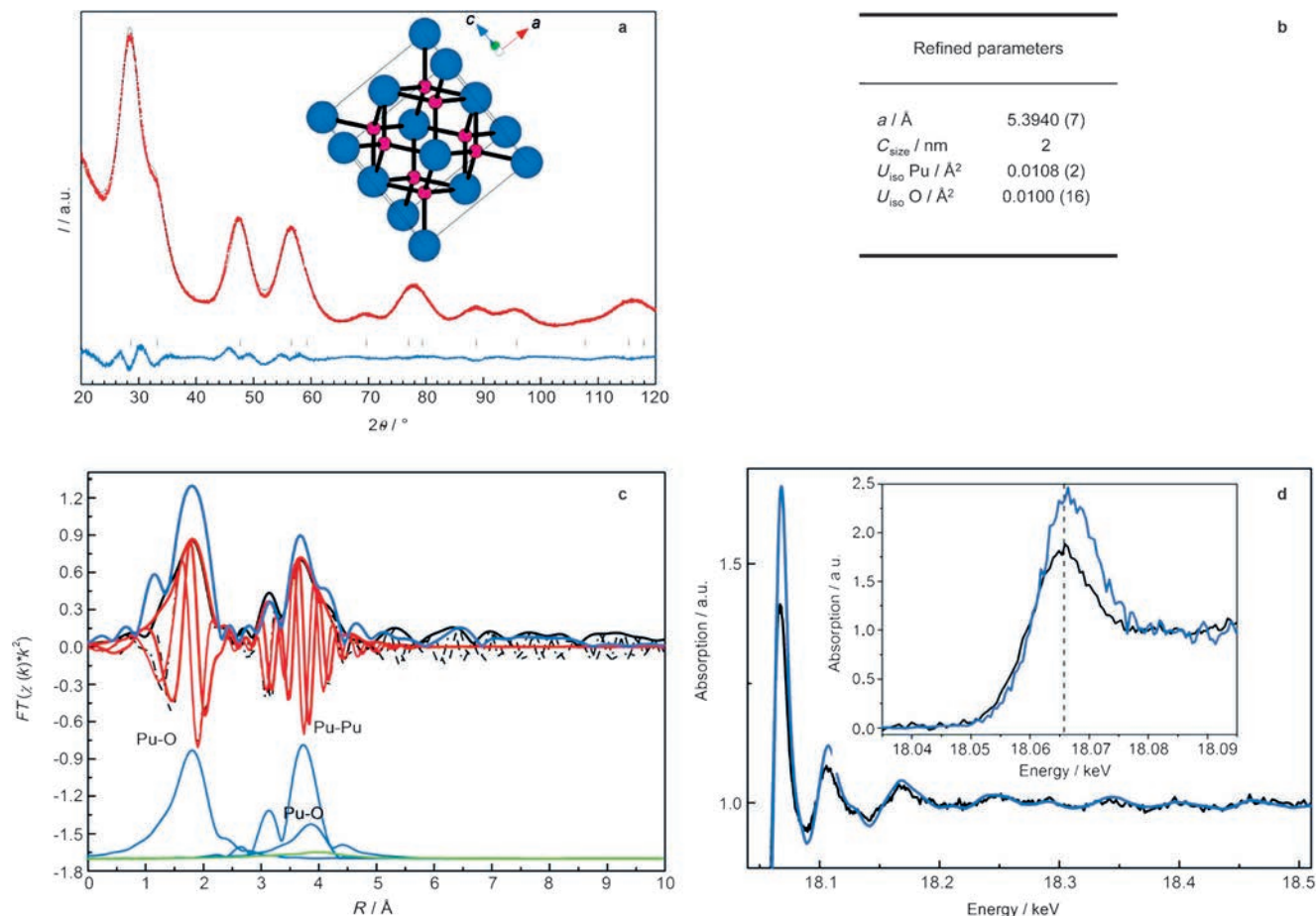


Figure 1. Structural characterization (PXRD and XAFS) of the PuO_2 nanocrystals synthesized through the heating up technique in a mixture of $[\text{PuO}_2(\text{NO}_3)_2] \cdot 3\text{H}_2\text{O}/\text{BnOBn}/\text{OA}/\text{OAm}$. a) Rietveld refinement of the room temperature PXRD data (values of reliability: GOF: 2.4, Rp: 2.95, Rwp: 3.79). Data points are shown (red spheres) with the fit (black solid line) and the difference curve (blue solid line). Tick marks indicate bulk PuO_2 Bragg peaks positions. The inset shows the crystallographic structure of the PuO_2 nanocrystals derived from the Rietveld refinement (plutonium and oxygen atoms are in blue and pink, respectively); b) Values obtained for the physical parameters which were refined (a = cell parameter, C_{size} = crystallite size, U_{iso} = isotropic atomic displacement parameter); c) Pu L_3 edge Fourier transformed extended X ray absorption fine structure (FT EXAFS) spectra of the as prepared PuO_2 NCs (black), its best fit (red), and bulk PuO_2 (violet). Vertically shifted are the contributions of the single (blue) and multiple scattering paths (green) used in the modelling; d) Pu L_3 edge X ray absorption fine structure (XAFS) spectra and high energy resolution x ray absorption near edge structure (HR XANES) spectra (inset) of the as prepared PuO_2 NCs (black) and bulk PuO_2 (violet).

mined by the Rietveld refinement, whereas the Pu–Pu distance ($3.81 \pm 0.01 \text{ \AA}$) matches within the error bar. The contribution of the strained Pu–O surface bonds account for shortening of the average Pu–O distance compared with bulk PuO_2 . It is worth pointing out that those deviations between PXRD and EXAFS are not unexpected in case of NCs. Indeed, the former measures an average crystal structure and small deviations from the average cannot be detected by classical PXRD,^[20] whereas the later measures a local structure and hence it is sensitive to the surface contribution.

The overall shape of the plutonium L_3 edge X-ray absorption fine structure (XAFS) spectrum of PuO_2 NCs in Figure 1d closely resembles the spectrum of bulk PuO_2 . The damping of the intensity of the post-edge features and lower intensity of the most intense absorption resonance at about 18.067 keV (white line, WL) can be attributed to the small size of the NCs. The scattering events are limited close to the surface and larger disorder compared to bulk PuO_2 might be present in the NCs.

The energy position of the maximum of the WL of the PuO_2 NCs XANES and high-energy resolution XANES (HR-XANES) spectra (Figure 1d and its inset, respectively) is shifted to lower energy ($0.9 \pm 0.25 \text{ eV}$) compared to the WL maximum of bulk PuO_2 . It has been shown by Conradson et al. that the bonding of ligands and geometric characteristics can largely influence the energy position of the WL.^[21] The authors reported up to 2 eV energy difference for Pu(IV) (Pu–O bonding in various materials). Therefore, it is likely that the detected energy shift is introduced by the plutonium atoms stabilized by organic ligands on the surface of the NCs (see the IR spectroscopic characterizations later).

Transmission electron microscopy

Although over the last decade several papers dealing with plutonium colloids were published, detailed analyses including high quality TEM data are scarce.^[12b] Such data are needed to

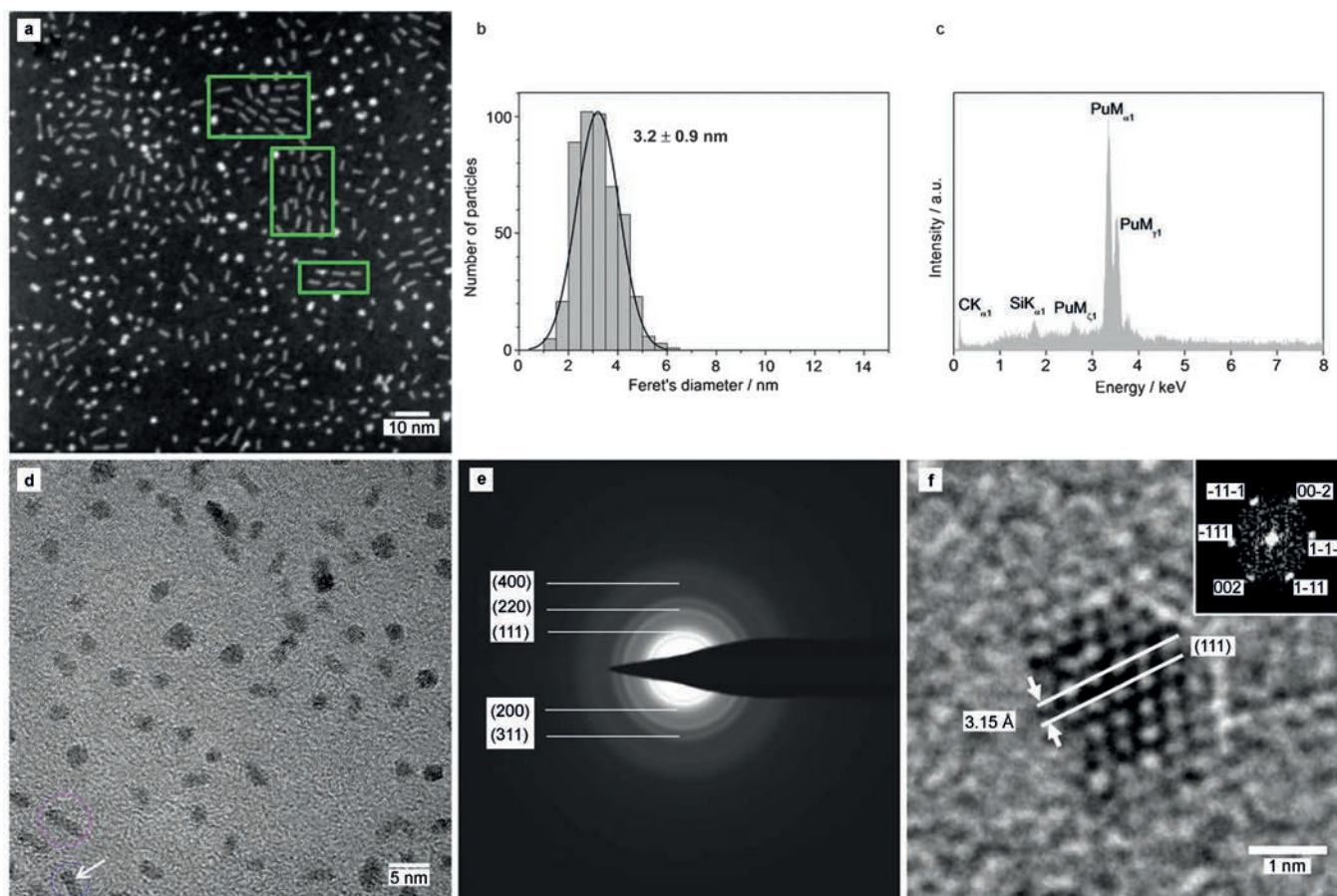


Figure 2. The panels show the full TEM characterization of the PuO_2 nanocrystals synthesized via the heating up technique in a mixture of $[\text{PuO}_2(\text{NO}_3)_2] \cdot 3\text{H}_2\text{O}$ /BnOBn/OA/OAm. The upper row shows the STEM image (a) as well as the corresponding size distribution (b) and the EDX spectrum (c). The lower row shows the TEM image (d) and its corresponding selected area electron diffraction pattern (e) as well as a high resolution image of an individual nanocrystal (f) and its corresponding FFT (inset).

fully characterize nano-objects and are complementary to the structural investigations that can be carried out by using PXRD or XAFS. Panels in Figure 2 show the scanning transmission electron microscopy (STEM) picture (Figure 2a) of the as-prepared PuO_2 NCs as well as the corresponding size distribution analysis (Figure 2b) and energy-dispersive X-ray (EDX) spectrum (Figure 2c). Additional panels show a transmission electron microscopy (TEM) picture (Figure 2d) and its corresponding selected area electron diffraction (SAED) pattern (Figure 2e) as well as a high-resolution transmission electron microscopy (HRTEM) picture (Figure 2f). Figure 2a shows that non-agglomerated ultra-small PuO_2 NCs were formed. Although the experiment with plutonyl nitrate was realized under similar experimental conditions as for uranyl and neptunyl nitrates,^[9] the results are different. First, it is obvious that two different kinds of population co-exist, namely nanodots (isotropic particles) and nanorods (anisotropic particles). Among the actinides and until now, the growth of anisotropic shapes was only reported for thorium. It clearly indicates that the nature of the actinide center and its associated chemistry play a significant role. Multiple growth mechanisms underlying the formation of NCs with different shapes can be influenced by different param-

eters.^[15d,22] Additional experiments are still needed to selectively grow purely isotropic or anisotropic PuO_2 NCs as for ThO_2 .^[8a]

In this first investigation, a size distribution analysis (Figure 2b) was carried out without any distinction between the two populations of PuO_2 NCs mainly because of the very small size of the two populations (see the Supporting Information for detailed explanations as well as Figures S3 and S4). The calculated average Feret diameter is (3.2 ± 0.9) nm. Within each of the two populations, the NCs are highly monodisperse. Indeed, the mean diameter of the isotropic NCs is around 2 nm, whereas the anisotropic NCs exhibit a highly monodisperse short axis (0.9 nm) and a slightly bigger dispersion of the long length axis with an average value around 4 nm. The EDX spectrum (Figure 2c) clearly shows that the NCs contain plutonium as the only heavy element. Lattice fringes are clearly visible from the TEM picture (Figure 2d) and are characteristic of highly crystalline materials (confirming the results obtained by PXRD and XAFS). Nanodots are single-domain whereas nanorods can be single- (pink circle, Figure 2d) or multi-domain (blue circle, Figure 2d). The existence of such multi-domains (the Supporting Information, Figure S5) could indicate the hypothesis of growth by the oriented attachment of smaller iso-

tropic particles.^[23] The SAED pattern is characteristic of a face-centered cubic (FCC) structure and is in good agreement with the one of bulk PuO₂ confirming the results obtained by PXRD. Some individual well-oriented NCs were particularly adapted for high-resolution imaging. A typical HRTEM picture of an individual PuO₂ NC is given in Figure 2f along with its corresponding FFT as an inset. The indexation of the latter is in good agreement with the bulk fluorite (fcc) structure and reveals the [110] direction as being the zone axis. Nevertheless, small deviations compared with the average structure determined by PXRD (i.e., surface contribution) cannot be excluded. Such behavior is common for NCs^[24] and EXAFS results indicated that surface effects are not negligible. Although ²³⁹Pu is a strong alpha emitter, the lattice fringes on the HRTEM picture clearly prove the high crystallinity of the PuO₂ NCs within a dimension as short as 2 nm. Such size is very close to the one recently reported for intrinsic plutonium colloids.^[12b-d] The measured distance of 3.15 Å is in relatively good agreement with the d₁₁₁ interplanar distance of bulk PuO₂. In addition to the X-ray based investigations and TEM characterizations, the as-pre-

pared PuO₂ NCs were characterized by various spectroscopic methods.

Spectroscopic investigations

The nature of the stabilizing ligand is easily detected by FTIR spectroscopy. Figure 3a shows the mid-IR spectrum of the as-prepared PuO₂ NCs and clearly indicates the presence of oleate anions (i.e., the carboxylate moiety).

Indeed, in the 2800–3000 cm⁻¹ region, characteristic vibrations of an alkyl chain are observed whereas the vibrations in the 1300–1700 cm⁻¹ region indicate the coordination of a carboxylate with a metal center. The absorption starting at about 650 cm⁻¹ is better described with the far-IR spectrum (Figure 3b). The latter is characterized by a broad absorption centered between 450 and 500 cm⁻¹ and a clearly distinguishable shoulder between 310 and 280 cm⁻¹. For comparison, a similar far-IR spectrum was recorded on bulk PuO₂ powders of micrometric crystallites (dotted curve in Figure 3b). The bulk PuO₂ sample was annealed for 8 h at 1800 K in air (the Supporting

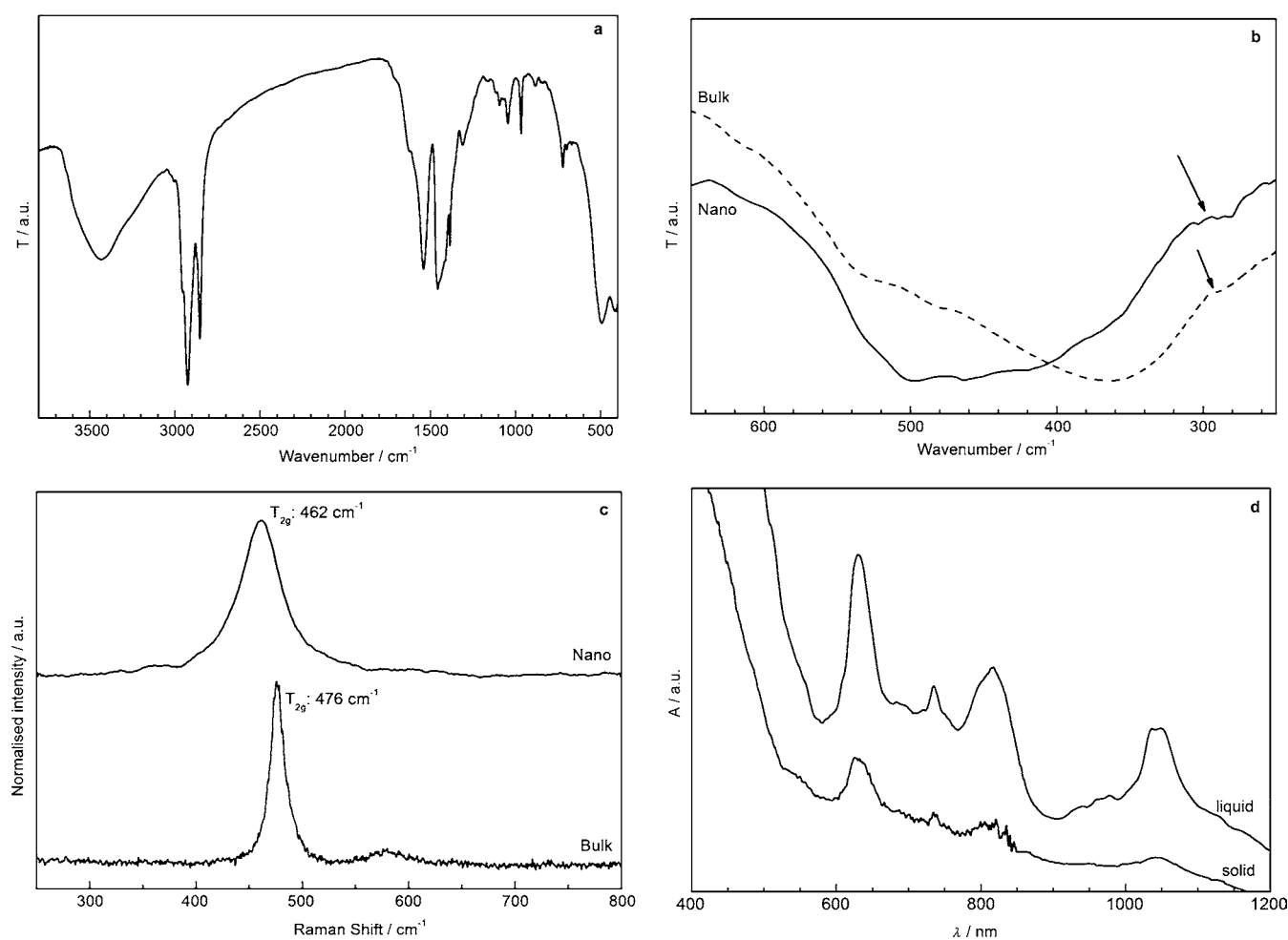


Figure 3. Spectroscopic characterization of the PuO₂ nanocrystals (NCs) synthesized through the heating up technique in a mixture of [PuO₂(NO₃)₂]-3H₂O/BnOBn/OA/OAm. a) Solid state mid infrared spectrum of PuO₂ NCs dispersed in a KBr matrix; b) Solid state far infrared spectra of bulk (dash line) and nano (solid line) PuO₂ dispersed in a polyethylene matrix; c) Solid state Raman spectra of a thin layer of PuO₂ NCs deposited onto an aluminum plate (top curve) and a bulk PuO₂ reference (bottom curve); d) Liquid state Vis NIR spectrum of PuO₂ NCs dispersed in toluene (liquid) and solid state Vis NIR spectrum of dried PuO₂ NCs (solid).

Information, Figure S6) to cure eventual self-irradiation effects, including the formation of oxygen defects.^[25] The general shape of the corresponding absorption spectrum is similar to the spectrum of PuO₂ NCs, however, with significant differences: 1) The broad band has a better defined maximum absorption at 360 cm⁻¹, and 2) the lower energy shoulder (arrows in Figure 3b) is narrower and centered at 290 cm⁻¹. Concerning the observed broad absorption, it was previously detected for various bulk AnO₂ (with An = Th, U, Np, Pu) and was explained as being a manifestation of the size-dependent frequency of long wavelength modes.^[26] This also explains well the difference in its shape and maximum absorption frequency between the micro- and nanocrystalline PuO₂. As for the absorption at about 290 cm⁻¹, it is typical of the transverse optic phonon associated to the T_{1u} vibration of the Pu–O bond, already predicted and observed in bulk PuO₂.^[27] According to the Group Theory, it is the only IR-active vibration of PuO₂.^[27] Broadening of this band in PuO₂ NCs is probably related to a phonon confinement effect in the NCs.^[28] A similar effect has been observed when using Raman spectroscopy, and was already detected in previous research on similar nanocrystalline compounds such as, for example, CeO₂^[29] and ThO₂.^[30]

When using Raman spectroscopy, the fundamental Raman-active T_{2g} mode^[27] (i.e., Pu–O symmetrical stretching) was clearly identified for microcrystalline bulk PuO₂ at (476 ± 2) cm⁻¹ (Figure 3c, bottom curve).^[31] In the as-prepared PuO₂ NCs (Figure 3c, top curve), the maximum of the T_{2g} peak is shifted to lower wavenumber (462 cm⁻¹) and the line width is significantly broadened (from 17 cm⁻¹ for bulk PuO₂ to 47 cm⁻¹ for PuO₂ NCs). The Brillouin zone Γ -edge intercepts of recently calculated optical phonon dispersion curves for UO₂ and PuO₂ slightly overestimate, for both compounds, the frequency of both T_{1u} and T_{2g} modes.^[32]

Nonetheless, qualitative agreement between the calculated phonon spectra and both the current and previous experimental results^[27,33] on bulk PuO₂ is more than acceptable. Therefore, the peak shift towards lower energy and broadening observed here in PuO₂ NCs can be interpreted as a phonon confinement effect qualitatively following the LO1 phonon dispersion curve calculated by Yin and Savrasov along the (0 0 ξ) direction.^[32] However, the very small average size of the PuO₂ NCs investigated in the present work does not permit any more quantitative interpretation of the current vibrational spectroscopy results in the light of phonon confinement of an elastic sphere model.^[28] The small particle size probably explains also the fact that a weak Raman band visible in bulk PuO₂ around 575 cm⁻¹, corresponding to the zero-momentum LO2 phonon calculated by Yin and Savrasov,^[32] is not clearly visible in PuO₂ NCs.

Finally, the Vis-NIR spectroscopy was interesting to compare the prepared NCs with the reported Pu(IV) colloids in the literature. The liquid and solid-state spectra (Figure 3d) of the as-prepared PuO₂ NCs are very similar. Hence, it clearly shows that the PuO₂ NCs are not disturbed when forming a stable colloidal suspension in toluene. Interestingly, the Vis-NIR spectrum of the as-prepared PuO₂ NCs are similar with the one of many Pu(IV) colloids reported by various authors.^[12a,c,d]

Hence, we can imagine that during the condensation process and the formation of intrinsic Pu(IV) colloids, ultra-small plutonium oxide NCs with a fluorite structure close to the one reported for bulk PuO₂ are formed although differences can be observed (depending on the experimental conditions) about their respective surface chemistry and degree of agglomeration.

Magnetic properties

From a fundamental point of view, the synthesized PuO₂ NCs give also the opportunity to enter into a domain in which size/shape effects are known to modify physical properties as widely observed with stable elements. As an example, the first results about magnetic properties of the synthesized PuO₂ NCs are reported. One important feature of bulk PuO₂ is the absence of a magnetic moment on the Pu atom despite the Pu(IV) electronic configuration that should lead to a Curie Weiss behavior. This surprising aspect has been first reported by a temperature-independent paramagnetic behavior (TIP) for the magnetic susceptibility^[34] and is still at the origin of numerous debates. The reduced dimensionality of the PuO₂ NCs could perturb the magnetic stability around Pu atoms at an atomic level. Hence, magnetization measurements have been performed on the as-prepared PuO₂ NCs. The first main point is a similar TIP behavior as observed for bulk PuO₂. Nevertheless, a slightly enhanced constant value of the magnetic susceptibility ($M/H(300\text{ K}) = \chi_{\text{DC}}(300\text{ K}) = 0.835 \cdot 10^{-3} \text{ emu mol}^{-1}$) is observed (Figure 4a). Whereas no hysteresis is observed between the zero-field cooled (ZFC) and field cooled (FC) curves, a very slight positive upturn is visible below 10 K that could be associated to defects due to the self-irradiation damage (the sample was measured 19 days after the synthesis). The second main point is that the system does not show any ferromagnetic features even at the lowest reached temperature (3 K). This behavior is similar to the one recently observed with thorium/uranium mixed oxide (Th_{1-x}U_xO₂ with 0 ≤ x ≤ 1) NCs^[14] as we observe a linear dependence of the magnetization versus field associated to a paramagnetic behavior.

Once again, this observation contradicts the recently reported results about universal ferromagnetism in non-magnetic metal^[35] or metal oxide^[36] NCs. Additionally, an interesting aspect is noticeable with a possible memory effect when varying the applied magnetic field above 10 kOe characterized by a magnetic loop opening (Figure 4b). This signature, characteristic of a memory effect, is quite puzzling as the global magnetic response of PuO₂ NCs (TIP and absence of hysteretic features) does not show similarities with recently reported nano-systems presenting a memory effect such as Ni₈₁Fe₁₉ or Fe₃N alloys.^[37] Because of the strong impact of self-irradiation damage on the material, the memory effect disappears within two weeks (Figure 4c), whereas the global magnetization curve remains unchanged. These first results show for the first time within the actinide series that the reduced dimensionality can modify physical properties (in that case magnetism) compared to the bulk counterpart.

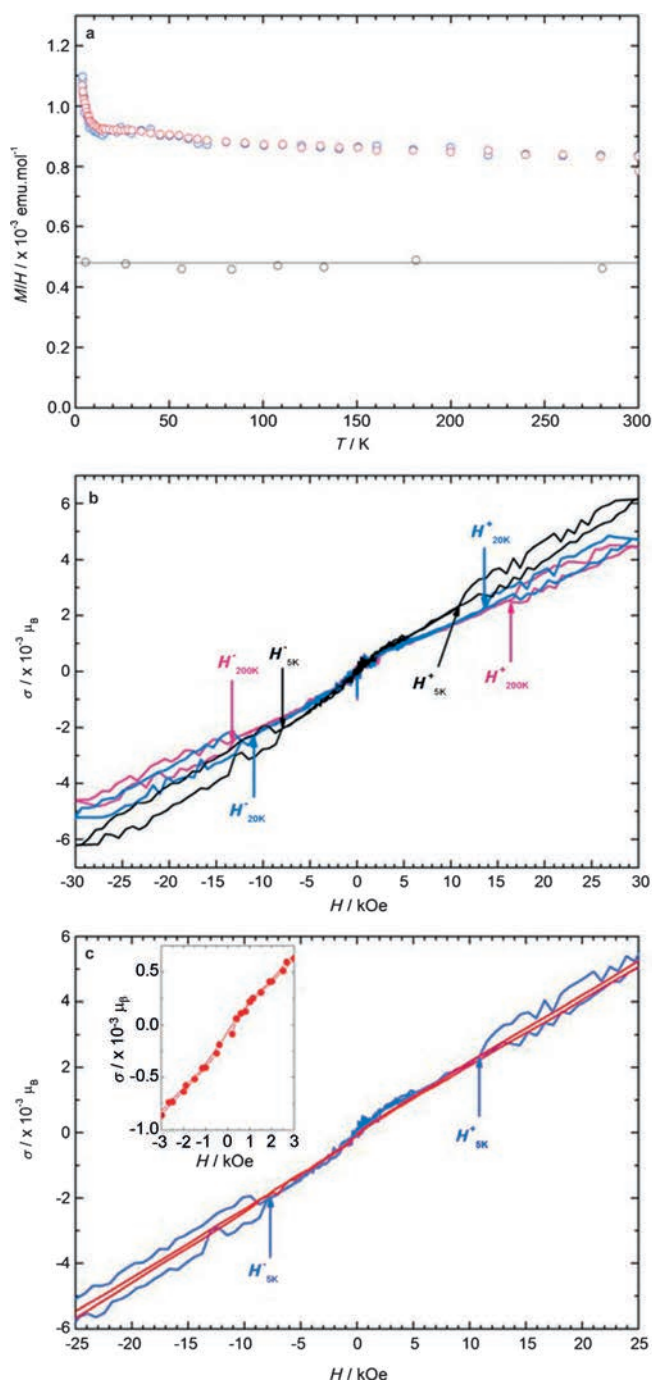


Figure 4. a) Magnetic susceptibility χ of PuO_2 NCs. Measurement versus temperature has been performed at 10 kOe (blue circles) and 30 kOe (red circles) from 300 K down to 3 K. Data reported for bulk PuO_2 are also shown (black circles); b) The field dependence of magnetization for the PuO_2 NCs at three different temperatures namely 5 K (black), 20 K (blue) and 200 K (pink). The hysteric loop opens at critical fields $H_T \approx 10.9, 13.5,$ and 16.3 kOe, respectively; c) The impact of aging on the as prepared PuO_2 NCs (violet) and the disappearance of the hysteric loop after two weeks (red).

Conclusion

The non-aqueous synthesis of actinide oxide NCs, whose efficiency is now demonstrated for the main actinides (i.e., ^{232}Th , $^{235/238}\text{U}$, ^{237}Np , and ^{239}Pu), is a new and powerful tool for acti-

nide chemistry at the nanoscale. The latter is unique when dealing with highly challenging transuranium elements and offers the possibility to design various model systems providing an unprecedented control over important parameters such as the chemical composition, the size and shape distributions, as well as the surface chemistry of actinide-based nanoscale building blocks.

In this work, we have demonstrated for the first time that ultra-small and highly crystalline PuO_2 NCs can be synthesized in a controllable manner. The first whole set of data (PXRD, XAFS, TEM, optical spectroscopy) related to the structural characterization of PuO_2 NCs was provided and clearly indicates the existence of the cubic FCC structure slightly disturbed due to surface effects. The results clearly demonstrated that despite the strong alpha activity of ^{239}Pu , PuO_2 NCs as small as two nanometers can be stabilized as nanodots and nanorods. From a practical point of view, highly crystalline PuO_2 NCs could constitute the backbone for the majority of the intrinsic Pu(IV) colloids reported in the literature within the last decades, although the corresponding surface chemistry is different. From a fundamental point of view, PuO_2 NCs exhibit unexpected magnetic features (possible memory effect) different compared to their bulk counterpart. Deep insights into the mechanisms governing the formation of PuO_2 NCs (as recently published with thorium and uranium oxides) are highly desirable and will pave the way to prepare highly monodisperse NCs that can be used to tackle challenging problems as diverse as the transport of plutonium in the environment or the influence of size and shape effects on the properties of 5f electrons.

Experimental Section

Syntheses

CAUTION!!! Because plutonium (^{239}Pu) is used in this study, usual precautions for working with radioactive materials should be followed. All experiments have been performed in dedicated gloveboxes within a dedicated nuclear facility (Institute for Transuranium Elements - ITU, Karlsruhe - Germany).

Synthesis of plutonium oxide NCs: The synthesis was performed using air-free techniques under purified argon atmosphere in a glovebox. $[\text{PuO}_2(\text{NO}_3)_2] \cdot 3\text{H}_2\text{O}$ (0.209 g, 0.5 mmol) is introduced in a previously degassed mixture of BnOBn (1500 μL , 7.87 mmol) and OA (1054 μL , 3.34 mmol). The resulting mixture was heated to 110°C for 10 min to dissolve $[\text{PuO}_2(\text{NO}_3)_2] \cdot 3\text{H}_2\text{O}$. The solution turned from yellowish to dark-red (the Supporting Information, Figure S1 a and S1 b) within a few minutes. When a clear dark-red solution was obtained, OAm was added (1700 μL , 5.15 mmol) (the Supporting Information, Figure S1 c). The resulting solution was degassed under vacuum at 110°C for 20 min. The mixture was then successively heated up ($10^\circ\text{C min}^{-1}$) to 220 and 280°C , and kept at each temperature for 30 min. During the thermal treatment, the mixture turned from dark-red to dark-green (the Supporting Information, Figure S1 d). Afterwards, the heating mantle was removed and the flask was left to cool naturally to room temperature.

Recovery and purification procedure of NCs

Absolute ethanol was added (at room temperature) to the thermally treated plutonium solution. The initial clear dark-green solution

floculates immediately (the Supporting Information, Figure S1 e). After centrifuging (4300 rpm, 20 min) the clear supernatant was discarded and the resulting olive-green precipitate was dispersed in toluene. This purification procedure (ethanol precipitation/centrifuging/toluene dispersion) was repeated three times to remove all residual organics. The extracted product is easily dispersible in apolar solvents such as toluene (the Supporting Information, Figure S1 f).

Characterization techniques

All details regarding the different characterization techniques are given in the Supporting Information.

Acknowledgements

Daniel Bouexiere is acknowledged for his help with powder X-ray diffraction measurements. We acknowledge the Synchrotron Light Source ANKA for provision of beamtime.

Keywords: controlled synthesis · magnetic properties · nanoparticles · plutonium · structural characterization

- [1] a) A. M. Boring, J. L. Smith, *Los Alamos Science* **2000**, 26, 90 127; b) J. M. Wills, O. Erikson, *Los Alamos Science* **2000**, 26, 128 151; c) R. C. Albers, *Nature* **2001**, 410, 759 761.
- [2] D. L. Clark, *Los Alamos Science* **2000**, 26, 364 381.
- [3] a) G. Hodes, *Adv. Mater.* **2007**, 19, 639 655; b) M. A. El Sayed, *Acc. Chem. Res.* **2004**, 37, 326 333; c) A. P. Alivisatos, *Endeavour* **1997**, 21, 56 60.
- [4] D. V. Talapin, J. S. Lee, M. V. Kovalenko, E. V. Shevchenko, *Chem. Rev.* **2010**, 110, 389 458.
- [5] O. E. Semonin, J. M. Luther, M. C. Beard, *Mater. Today* **2012**, 15, 508 515.
- [6] D. C. Lee, D. K. Smith, A. T. Heitsch, B. A. Korgel, *Annu. Rep. Prog. Chem. C* **2007**, 103, 351 402.
- [7] X. Wang, L. Yang, Z. Chen, D. M. Shin, *Ca Cancer J. Clin.* **2008**, 58, 97 110.
- [8] a) D. Hudry, C. Apostolidis, O. Walter, T. Gouder, E. Courtois, C. Kübel, D. Meyer, *Chem. Eur. J.* **2013**, 19, 5297 5305; b) D. Hudry, C. Apostolidis, O. Walter, T. Gouder, E. Courtois, C. Kübel, D. Meyer, *Chem. Eur. J.* **2012**, 18, 8283 8287; c) G. Rousseau, M. Fattahi, B. Grambow, L. Desgranges, F. Boucher, G. Ouvrard, N. Millot, J. C. Niepce, *J. Solid State Chem.* **2009**, 182, 2591 2597; d) Q. Wang, G. D. Li, S. Xu, J. X. Li, J. S. Chen, *J. Mater. Chem.* **2008**, 18, 1146 1152; e) D. Kumar, G. K. Dey, N. M. Gupta, *Phys. Chem. Chem. Phys.* **2003**, 5, 5477 5484; f) Z. T. Zhang, M. Konduru, S. Dai, S. H. Overbury, *Chem. Commun.* **2002**, 2406 2407; g) H. M. Wu, Y. G. Yang, Y. C. Cao, *J. Am. Chem. Soc.* **2006**, 128, 16522 16523.
- [9] D. Hudry, C. Apostolidis, O. Walter, T. Gouder, A. Janssen, E. Courtois, C. Kübel, D. Meyer, *RSC Adv.* **2013**, 3, 18271 18274.
- [10] a) A. P. Novikov, S. N. Kalmykov, S. Utsunomiya, R. C. Ewing, F. Horreard, A. Merkulov, S. B. Clark, V. V. Tkachev, B. F. Myasoedov, *Science* **2006**, 314, 638 641; b) A. B. Kersting, D. W. Efurud, D. L. Finnegan, D. J. Rokop, D. K. Smith, J. L. Thompson, *Nature* **1999**, 397, 56 59.
- [11] A. B. Kersting, *Inorg. Chem.* **2013**, 52, 3533 3546.
- [12] a) A. I. Abdel Fattah, D. Zhou, H. Boukhalfa, S. Tarimala, S. D. Ware, A. A. Keller, *Environ. Sci. Technol.* **2013**, 47, 5626 5634; b) B. A. Powell, Z. Dai, M. Zavarin, P. Zhao, A. B. Kersting, *Environ. Sci. Technol.* **2011**, 45, 2698 2703; c) R. E. Wilson, S. Skanthakumar, L. Soderholm, *Angew. Chem.* **2011**, 123, 11430 11433; *Angew. Chem. Int. Ed.* **2011**, 50, 11234 11237; d) L. Soderholm, P. M. Almond, S. Skanthakumar, R. E. Wilson, P. C. Burns, *Angew. Chem.* **2008**, 120, 304 308; *Angew. Chem. Int. Ed.* **2008**, 47, 298 302.
- [13] a) C. B. Murray, C. R. Kagan, M. G. Bawendi, *Annu. Rev. Mater. Sci.* **2000**, 30, 545 610; b) J. Park, J. Joo, S. G. Kwon, Y. Jang, T. Hyeon, *Angew. Chem.* **2007**, 119, 4714 4745; *Angew. Chem. Int. Ed.* **2007**, 46, 4630 4660.
- [14] D. Hudry, J. C. Griveau, C. Apostolidis, O. Walter, E. Colineau, G. Rasmusen, D. Wang, V. S. K. Chakravadhanula, E. Courtois, C. Kübel, D. Meyer, *Nano Res.* **2014**, 7, 119 131.
- [15] a) J. w. Seo, Y. w. Jun, S. J. Ko, J. Cheon, *J. Phys. Chem. B* **2005**, 109, 5389 5391; b) R. Buonsanti, E. Carlino, C. Giannini, D. Altamura, L. De Marco, R. Giannuzzi, M. Manca, G. Gigli, P. D. Cozzoli, *J. Am. Chem. Soc.* **2011**, 133, 19216 19239; c) R. Buonsanti, V. Grillo, E. Carlino, C. Giannini, T. Kipp, R. Cingolani, P. D. Cozzoli, *J. Am. Chem. Soc.* **2008**, 130, 11223 11233; d) Y. W. Jun, J. S. Choi, J. Cheon, *Angew. Chem.* **2006**, 118, 3492 3517; *Angew. Chem. Int. Ed.* **2006**, 45, 3414 3439.
- [16] D. L. Clark, S. S. Hecker, G. D. Jarvinen, M. P. Neu, *The Chemistry of the Actinide and Transactinide Elements*, Springer, Dordrecht, **2006**, p.1395.
- [17] a) R. W. Cheary, A. A. Coelho, *J. Appl. Crystallogr.* **1998**, 31, 851 861; b) R. W. Cheary, A. A. Coelho, *J. Appl. Cryst.* **1998**, 31, 862 868.
- [18] J. M. Haschke, *Science* **2000**, 287, 285 287.
- [19] a) S. D. Conradson, B. D. Begg, D. L. Clark, C. Den Auwer, M. Ding, P. K. Dorhout, F. J. Espinosa Faller, P. L. Gordon, R. G. Haire, N. J. Hess, R. F. Hess, D. W. Keogh, G. H. Lander, D. Manara, L. A. Morales, M. P. Neu, P. Paviet Hartmann, J. Rebizant, V. V. Rondinella, W. Runde, C. D. Tait, D. K. Veirs, P. M. Vilella, F. Wastin, *J. Solid State Chem.* **2005**, 178, 521 535; b) S. D. Conradson, B. D. Begg, D. L. Clark, C. den Auwer, M. Ding, P. K. Dorhout, F. J. Espinosa Faller, P. L. Gordon, R. G. Haire, N. J. Hess, R. F. Hess, D. W. Keogh, L. A. Morales, M. P. Neu, P. Paviet Hartmann, W. Runde, C. D. Tait, D. K. Veirs, P. M. Vilella, *J. Am. Chem. Soc.* **2004**, 126, 13443 13458; c) S. D. Conradson, B. D. Begg, D. L. Clark, C. Den Auwer, F. J. Espinosa Faller, P. L. Gordon, N. J. Hess, R. Hess, D. W. Keogh, L. A. Morales, M. P. Neu, W. Runde, C. D. Tait, D. K. Veirs, P. M. Vilella, *Inorg. Chem.* **2003**, 42, 3715 3717; d) P. Martin, S. Grandjean, M. Ripert, M. Freyss, P. Blanc, T. Petit, *J. Nucl. Mater.* **2003**, 320, 138 141.
- [20] S. J. L. Billinge, I. Levin, *Science* **2007**, 316, 561 565.
- [21] S. D. Conradson, K. D. Abney, B. D. Begg, E. D. Brady, D. L. Clark, C. den Auwer, M. Ding, P. K. Dorhout, F. J. Espinosa Faller, P. L. Gordon, R. G. Haire, N. J. Hess, R. F. Hess, D. W. Keogh, G. H. Lander, A. J. Lupinetti, L. A. Morales, M. P. Neu, P. D. Palmer, P. Paviet Hartmann, S. D. Reilly, W. H. Runde, C. D. Tait, D. K. Veirs, F. Wastin, *Inorg. Chem.* **2003**, 42, 116 131.
- [22] Y. W. Jun, J. H. Lee, J. S. Choi, J. Cheon, *J. Phys. Chem. B* **2005**, 109, 14795 14806.
- [23] C. J. Dalmaschio, C. Ribeiro, E. R. Leite, *Nanoscale* **2010**, 2, 2336 2345.
- [24] S. J. L. Billinge, *J. Solid State Chem.* **2008**, 181, 1695 1700.
- [25] R. Böhler, M. J. Welland, D. Prieur, P. Cakir, T. Vitova, T. Pruessmann, I. Pidchenko, C. Hennig, C. Guéneau, R. J. M. Konings, D. Manara, *J. Nucl. Mater.* **2014**, 448, 330 339.
- [26] J. D. Axe, G. D. Pettit, *Phys. Rev.* **1966**, 151, 676 680.
- [27] L. Manes, A. Barisich, *Phys. Status Solidi A* **1970**, 3, 971 981.
- [28] G. Gouadec, P. Colomban, *Prog. Cryst. Growth Charact. Mater.* **2007**, 53, 1 56.
- [29] I. Kosacki, T. Suzuki, H. U. Anderson, P. Colomban, *Solid State Ionics* **2002**, 149, 99 105.
- [30] M. Rajalakshmi, A. K. Arora, S. Dash, A. K. Tyagi, *J. Nanosci. Nanotechnol.* **2003**, 3, 420 422.
- [31] M. J. Sarsfield, R. J. Taylor, C. Puxley, H. M. Steele, *J. Nucl. Mater.* **2012**, 427, 333 342.
- [32] Q. Yin, S. Y. Savrasov, *Phys. Rev. Lett.* **2008**, 100, 225504.
- [33] G. M. Begun, R. G. Haire, W. R. Wilmarth, J. R. Peterson, *Journal of the Less Common Metals* **1990**, 162, 129 133.
- [34] G. Raphael, R. Lallement, *Solid State Commun.* **1968**, 6, 383 385.
- [35] V. Tuboltsev, A. Savin, A. Pirojenko, J. Räisänen, *ACS Nano* **2013**, 7, 6691 6699.
- [36] a) A. Sundaresan, C. N. R. Rao, *Nano Today* **2009**, 4, 96 106; b) A. Sun darsan, R. Bhargavi, N. Rangarajan, U. Siddesh, C. N. R. Rao, *Phys. Rev. B* **2006**, 74, 161306.
- [37] a) Y. Sun, M. B. Salamon, K. Garnier, R. S. Averback, *Phys. Rev. Lett.* **2003**, 91, 167206; b) M. Sasaki, P. E. Jönsson, H. Takayama, H. Mamiya, *Phys. Rev. B* **2005**, 71, 104405.

Repository KITopen

Dies ist ein Postprint/begutachtetes Manuskript.

Empfohlene Zitierung:

Hudry, D.; Apostolidis, C.; Walter, O.; Janen, A.; Manara, D.; Griveau, J. C.; Colineau, E.; Vitova, T.; Prüßmann, T.; Wang, D.; Kübel, C.; Meyer, D.
[Ultra-small plutonium oxide nanocrystals: An innovative material in plutonium science](#)
2014. Chemistry - a European journal, 20, 10431–10438.
[doi:10.5445/IR/110097435](https://doi.org/10.5445/IR/110097435)

Zitierung der Originalveröffentlichung:

Hudry, D.; Apostolidis, C.; Walter, O.; Janen, A.; Manara, D.; Griveau, J. C.; Colineau, E.; Vitova, T.; Prüßmann, T.; Wang, D.; Kübel, C.; Meyer, D.
[Ultra-small plutonium oxide nanocrystals: An innovative material in plutonium science](#)
2014. Chemistry - a European journal, 20, 10431–10438.
[doi:10.1002/chem.201402008](https://doi.org/10.1002/chem.201402008)

Lizenzinformationen: [KITopen-Lizenz](#)